Calcul de l'élasticité anisotrope de l'os cortical à partir d'images quantitatives de microscopie acoustique

Quentin Grimal, Kay Raum, Alf Gerisch, Pascal Laugier

Computation of the overall anisotropic elasticity of cortical bone from micro-scale quantitative acoustic images

Calcul de l'élasticité anisotrope de l'os cortical à partir d'images quantitatives de microscopie acoustique

Quentin GRIMAL*†, Kay RAUM‡, Alf GERISCH‡‡ and Pascal LAUGIER†

†Université Pierre et Marie Curie-Paris6, Laboratoire d'Imagerie Paramétrique, Paris, F-75005 France; CNRS, LIP, Paris, F-75006 France
**Corresponding author.*
‡ Q-BAM Group, Dept. of Orthopedics
Martin-Luther-Universität Halle-Wittenberg, Magdeburger Straße 22, 06097 Halle (Saale), Germany
‡‡ Institut für Mathematik
Martin-Luther-Universität Halle-Wittenberg, Postfach D-06099 Halle (Saale), Germany

Résumé :

L'objectif de ce travail est présenter une méthode pour le calcul des constantes d'élasticité anisotropes de l'os cortical à partir d'images quantitatives à l'échelle microscopique. Des images, de résolution 23 μm, d'une section de radius humain sont obtenues avec un microscope acoustique. Les propriétés effectives de 58 réalisations d'échantillons millimétriques générées à partir des images de microscopie sont calculées en résolvant par la méthode des éléments finis des problèmes aux limites à déplacements imposés. Les propriétés millimétriques effectives obtenues sont dans la gamme des valeurs habituellement mesurées à cette échelle. A partir des constantes calculées, il est possible de déterminer des relations empiriques reliant les propriétés microscopiques (porosité, élasticité moyenne de la matrice osseuse) aux propriétés effectives. Le modèle développé est adapté non seulement à la prédiction de l'élasticité millimétrique à partir d'images micro mais également à l'étude des facteurs microscopiques constitutifs de l'élasticité osseuse effective.

Abstract :

The aim of the present work is to present a method to compute the anisotropic elastic parameters of cortical bone from quantitative images at the micro-scale. Images with 23 μm resolution are obtained with a 50-MHz acoustic microscope. The effective properties of 58 realizations of millimetre-scale samples generated from the images are computed upon solving the boundary value problem (imposed displacements) with the finite element method. The effective properties computed are in the range of the properties usually measured at the millimetre scale. From the computed values, it is possible to determine empiric relationships between the microscopic properties (porosity, average elasticity of the bone matrix) and the effective properties. The developed model is not only useful to estimate elasticity at the millimetre scale from micro-scale images but also to study the micro-scale factors which contribute to the effective bone elasticity.

Mots-clefs : Bone ; elasticity ; homogenization

1 Introduction

A good understanding of the bone material properties at the millimetre scale is important in the context of many applications in the field of orthopaedic surgery and management of bone pathologies. Furthermore, in personalized finite element models of bones at the organ level, one needs to provide mechanical properties at the millimetre scale, which is about the typical mesh

size. The millimetre scale is the continuum level relevant for an analysis at the organ level in the framework of continuum mechanics: a volume of $1\,\mathrm{mm}^3$ appears to contain several microstructural units (osteon) of cortical bone. Accordingly, the term 'mesoscopic' will be used throughout the paper to refer to the millimetre scale in cortical bone.

Bone mechanical properties depend on both the microstructure (shape and dimensions of the pores) and on the intrinsic material properties of the bone material. Cortical bone is a compact tissue with a porosity varying between a few percent and up to about 15 % [1]. The local anisotropic elastic properties of the bone matrix are essentially a result of specific arrangements of the mineralized collagen fibrils.

The motivation of the present work is to introduce a versatile tool to analyse micro-meso relationships in cortical bone. For this purpose, a finite element model of characteristic mesoscale volumes coupled with a high resolution quantitative imaging technique is proposed. This paper is focused on the relationships between porosity and elasticity at the millimetre scale.

2 Method

The geometry of the diaphysis of long bones can be modelled as a hollow cylinder. Let *O* denote a point of the cylinder axis. We will use the local reference Cartesian frame $R(O,\mathbf{x_1},\mathbf{x_2},\mathbf{x_3})$, where *O* is the origin of the Cartesian coordinate system and $(\mathbf{x_1},\mathbf{x_2},\mathbf{x_3})$ is an orthonormal basis where $\mathbf{x_3}$ is oriented in the direction of the cylinder axis and $\mathbf{x}_1$ and $\mathbf{x}_2$ are chosen arbitrarily in the plane normal to $\mathbf{x_3}$. Particle displacement is denoted by **u**, with coordinates (u_1,u_2,u_3) in the reference frame *R*.

Bone properties are investigated in the framework of linear elasticity. The components of the Cauchy stress tensor are denoted σ_{ij} and the components of the infinitesimal strain tensor are

$\varepsilon_{ij}=\frac{1}{2}\left(\frac{\partial u_i}{\partial x_j}+\frac{\partial u_j}{\partial x_i}\right)$. The generalized Hooke's law is $\sigma_{ij}=C_{ijkl}\varepsilon_{kl}$, where C_{ijkl} denote the components of the stiffness tensor of rank four. The so-called tensorial basis matrix representation is used in the present paper [2] to avoid manipulation of fourth rank tensors.

The effective elastic response of the heterogeneous material is then given by a relation between averages:

$$<[\sigma]>_\Omega=[C^*]<[\varepsilon]>_\Omega, \qquad (6)$$

where $<.>_\Omega=\frac{1}{|\Omega|}\int_\Omega .\,d\Omega$ is the average of the quantity between brackets over a statistically representative volume element (RVE) of volume $|\Omega|$ with characteristic dimension *L*, and $[C^*]$ is, by definition, the effective stiffness tensor [3]. In other words, $[C^*]$ is the stiffness tensor of an equivalent homogeneous material that fulfills the elastic deformation characteristics of the heterogeneous material in the sense of equation (6).

Microscopic data

An acoustic impedance image of a fresh human radius section cut in the $(\mathbf{x_1},\mathbf{x_2})$-plane was obtained with a 50-MHz scanning acoustic microscope. The sample preparation and experimental procedure have been reported elsewhere [4]. The spatial resolution of the image was 23 µm and the spatial increment between two adjacent image pixels was set to 20 µm.

Hence the image consists of a number of pixels with coordinates (x_1, x_2), each representing a 20×20 µm^2 surface. A calibration procedure was applied to convert the reflectivity signal into acoustical impedance values [5]. The pixel value is then directly related to the acoustic impedance of the material within the pixel area.

Fifty-eight RVE realizations $\theta_1, \theta_2 \cdots \theta_i \cdots \theta_{58}$ of the microscopic data were generated using the impedance spatial distribution of the entire radius section. The impedance data for one realization θ_i is an ensemble of values, denoted $Z(\theta_i; x_1, x_2)$, given at points $\mathrm{M}(x_1, x_2)$ which lie within a square of side length L=1 mm, where L is the mesoscale characteristic dimension. The square domains were selected manually on the radius cross section as shown in figure 1.

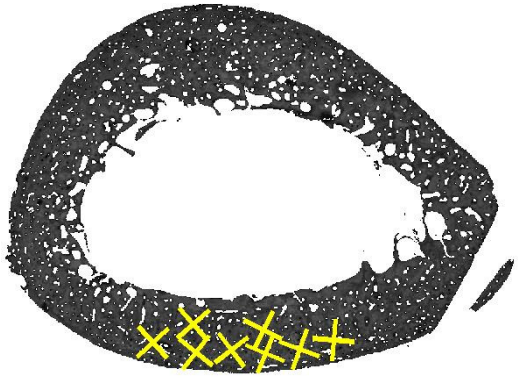

Figure 1: An example of the selection of eight mesoscopic RVE realizations in a cortical bone image obtained with a 50 MHz scanning acoustic microscope. Each cross represents the diagonals of a square RVE of side length 1 mm.

In a previous work, a threshold impedance value was determined which allows the segmentation of the pores (impedance values below 5 Mrayl) from the bone matrix [4]. After thresholding, the RVE can be seen as a composite material made of a heterogeneous bone matrix and pores. Considering the spatial resolution and pixel size, only the Haversian pores and resorption cavities can be separated from the rest of the tissue. Smaller pores—osteocytes lacunae, Volkman canals and canaliculi—cannot be resolved with the resolution of the device used. The mean porosity (relative area of pores *v.s.* total RVE area) of the population of 58 RVE realizations was 9.6 % with a standard deviation of 2.8 %.

In order to compute the 21 coefficients of the effective stiffness matrix $[C^*(\theta_i)]$ for one realization of the microscopic data, a three-dimensional (3D) RVE is constructed from the two-dimensional (2D) spatial distribution of impedance. For this purpose, we assumed that the microscopic data in the $\mathbf{x_3}$-direction is invariant. Finally, the impedance data for one RVE realization θ_i is an ensemble of values, denoted $Z(\theta_i; x_1, x_2, x_3)$, given at points $\mathrm{M}(x_1, x_2, x_3)$ which lie within a parallelepiped of volume $1 \times 1 \times d_3$ mm^3.

Impedance values $Z(x_1, x_2, x_3)$ *of the bone matrix* were converted to stiffness values $C_{33}^{\exp}(x_1, x_2, x_3)$ using an empirical law derived in a previous work [6]
$C_{33}^{\exp}(x_1, x_2, x_3) = 1.31 + 0.075 \cdot Z(x_1, x_2, x_3) + 0.5 \cdot Z^2(x_1, x_2, x_3)$, where the superscript 'exp' refers to the experimental nature of the stiffness values. A micromechanical model of the bone matrix proposed by Hellmich *et al.* [7] (referred to as 'Concept I' in the cited paper) was used in association with the values $C_{33}^{\exp}(x_1, x_2, x_3)$ in order to build a transverse isotropic

material model for the bone matrix. The mean value of $C_{33}^{\exp}(x_1, x_2, x_3)$ for the population of 58 RVE is 30.25 Gpa (SD 1.42 Gpa). The pores were considered to be filled with water. More details on the construction of the bone model are given in [8].

Finite element computations

The computation of effective properties consist in applying six sets of displacements boundary conditions [3] to the RVE. Computations were performed with a commercially available finite element program (Comsol Multiphysics© v3.2, Comsol France, Grenoble, France). The effective stiffness tensor obtained is then post-processed in order to find the closest stiffness tensor corresponding to hexagonal symmetry, which is the common symmetry assumption for human cortical bone; this was performed following a procedure described in [9] and using the software SYMETRIC (Marc François, LMT-Cachan, France).

2. Results and discussion

The computed mean values of the stiffness coefficients over the 58 mesoscopic volumes realizations are reported in Table 1. The values obtained for the stiffness coefficients in the present work are in the range of those measured with traditional ultrasonic methods in the MHz-range on cubes of volume several mm^3 [10-12].

Table 1 Mean effective stiffness properties computed.

	GPa	(SD)
C_{11}	**19.7**	1.98
C_{33}	**27.32**	3.13
C_{12}	**8.76**	0.73
C_{13}	**8.88**	1.87
C_{44}	**4.91**	0.94
C_{66}	**5.47**	0.67

Figure 2 shows the evolution of the values of some effective elastic properties with porosity. The following linear regressions are obtained, $E_1 = -0.55p + 20$ GPa (R^2=0.89); $E_3 = -0.39p + 25$ GPa (R^2 =0.51); $G_{13} = -0.31p + 7.9$ GPa (R^2=0.89), where p is the porosity (%).

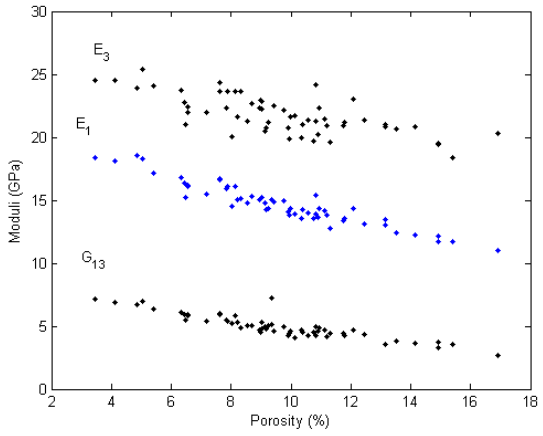

Figure 2 Elastic coefficients vs porosity for the 58 mesoscopic realizations

For a given porosity level, the dispersion in mesoscopic bone properties manifest in Fig. 2 is not only due to the variation of the microstructural parameters (pore shapes) within the cortical sample but also to the variations of elasticity of the bone matrix from one sample to another. In particular, the correlation coefficient between E_1 and the average value of the local $C_{33}^{\exp}$ is significant (R^2=0.34). In order to illustrate further this dependence, the mesoscopic properties for the 58 microstructure realizations were computed for mesoscopic samples having all the same bone matrix properties, namely $C_{33}^{\exp}$ =30.28 GPa. As a result, the mesoscopic samples considered only differed in their microstructure (porosity and shape of pores) and had homogeneous elastic properties. Figure 3 shows the values of E_1 obtained from the computations for the heterogeneous elasticity group (same values that appear in Fig. 2) and for the group with homogeneous elasticity. The indicator chosen to test the dispersion of the properties is again the linear correlation coefficient between mechanical properties and the porosity. The following correlation coefficients between E_1 and porosity are found: R=-0.945 (-0.909 –0.967) for the group with heterogeneous elasticity and R=-0.978 (-0.961 -0.986) for the group with homogeneous elasticity (the values in parenthesis are the 25 % and 75 % confidence intervals for the regression coefficients). The comparison of the correlation coefficients and the confidence intervals confirm that the dispersion of the Young moduli is in part due to variations in bone matrix elasticity. The rest of the dispersion is due to the pores' shapes.

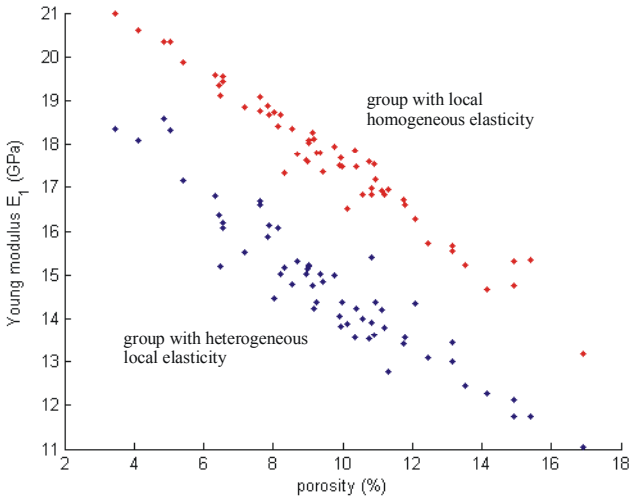

Figure 3 Young modulus in the transverse plane (E_1) vs. porosity. Blue: group with heterogeneous elasticity (same values as in Fig. 2); red: group with homogeneous elasticity values.

3. Conclusion

A method which combine a numerical model of cortical bone tissue and high resolution quantitative acoustical measurements has been introduced. The results presented in this proceeding show that the method has the potential to elucidate micro-macro relationships in bone, in particular the contribution of porosity and anisotropic matrix elasticity to the overall elastic bone properties.

Acknowledgements

The authors are indebted to Marc François (Université Pierre et Marie Curie-Paris6, LMT, Cachan, France) for helpful discussions on anisotropy and for providing the software SYMETRIC.

The authors are grateful for the financial supports to: Université Pierre et Marie Curie-Paris6 (BQR funding of the project "Modélisation mécanique du tissu osseux"); and the French-German research network "Ultrasound assessment of bone strength from the tissue level to the organ level" (DFG: Grant Ra 1380/1-1; CNRS).

References

1. Currey, J.D., 2002. *Bones: Structure and mechanics*: Princeton Academic Press.
2. Helnwein, P., 2001. *Some remarks on the compressed matrix representation of symmetric second-order and fourth-order tensors.* Computer Methods in Applied Mechanics and Engineering, **190**(22-23): p. 2753-2770.
3. Zohdi, T.I. and Wriggers, P., 2005. *Introduction to computational micromechanics*. Lecture notes in applied computational mechanics, ed. F. Pfeiffer and P. Wriggers. Berlin: Springer-Verlag.
4. Raum, K., Leguerney, I., Chandelier, F., Bossy, E., Talmant, M., Saied, A., Peyrin, F., and Laugier, P., 2005. *Bone microstructure and elastic tissue properties are reflected in qus axial transmission measurements.* Ultrasound in Medicine and Biology, **31**(9): p. 1225-1235.
5. Raum, K., Reisshauer, J., and Brandt, J., 2004. *Frequency and resolution dependence of the anisotropic impedance estimation in cortical bone using time-resolved scanning acoustic microscopy.* Journal of Biomedical Materials Research, **71A**(3): p. 430-438.
6. Raum, K., Cleveland, R.O., Peyrin, F., and Laugier, P., 2006. *Derivation of elastic stiffness from site-matched mineral density and acoustic impedance maps.* Physics in Medicine and Biology, **51**(3): p. 747-758.
7. Hellmich, C., Barthelemy, J.-F., and Dormieux, L., 2004. *Mineral-collagen interactions in elasticity of bone ultrastructure - a continuum micromechanics approach.* European Journal of Mechanics - A/Solids, **23**(5): p. 783-810.
8. Grimal, Q., Raum, K., Gerisch, A., and Laugier, P., 2007. *Derivation of the mesoscopic elasticity tensor of cortical bone from quantitative impedance images at the micron scale.* submitted to Computer Methods in Biomechanics and Biomedical Engineering.
9. François, M., Geymonat, G., and Berthaud, Y., 1998. *Determination of the symmetries of an experimentally determined stiffness tensor: Application to acoustic measurements.* International Journal of Solids and Structures, **35**(31-32): p. 4091-4106.
10. Yoon, H.S. and Katz, J.L., 1976. *Ultrasonic wave propagation in human cortical bone--ii. Measurements of elastic properties and microhardness.* Journal of Biomechanics, **9**(7): p. 459-464.
11. Rho, J.Y., 1996. *An ultrasonic method for measuring the elastic properties of human tibial cortical and cancellous bone.* Ultrasonics, **34**(8): p. 777-783.
12. Ashman, R.B., Cowin, S.C., van Buskirk, W.C., and Rice, J.C., 1984. *A continuous wave technique for the measurement of the elastic properties of cortical bone.* Journal of Biomechanics, **17**(5): p. 349-361.